Current-voltage characterization and 3D device modelling of p-type induced junction photodiode; surface recombination velocity and bulk lifetime

Chi Kwong Tang, Marit Ulset Nordsveen and Jarle Gran
Justervesenet (Norwegian Metrology Service)
Kjeller, Norway
Email: ckt@justervesenet.no

***Abstract*—A p-type silicon-based induced junction photodiode has been investigated with current-voltage (I-V) measurement under laser illumination at multiple power levels, and the results are fitted using 3D device simulations. When considering multiple laser power levels, it is found that material parameters that limit the performance of the photodiode can be extracted through fitting of a small voltage region of the I-V measurement.**

I. Introduction

Predictable Quantum Efficient Detector (PQED) is a detector-based primary standard for optical power [1]. It consists of two induced junction photodiodes in a trap configuration that minimizes the external losses to a negligible level [2]. The internal losses are predicted numerically with material parameters that are mainly based on manufacture values and measured values during the photodiode processing [3]. For the performance-limiting material parameters, it is essential to have non-destructive characterization methods to determine their values at the photodiode state (rather than at the wafer state) in order to monitor and compensate for variations. In our previous work with atomic layer deposited aluminum oxide on n-type silicon substrate [3], the oxide charge density (Q_f) and the surface recombination velocity (SRV) for electrons and holes were fitted to current-voltage (I-V) measurements. This enabled the extraction of the responsivity of the PQED. It was performed for one laser power level.

In this work, we show that the fitting strategy used in Ref.[3] can be simplified in our p-type silicon-based photodiode by only considering a small voltage region in I-V curves. In addition, multiple laser power levels are used to further strengthen the determination of the material parameters and, thereby, the responsivity of the induced junction photodiode.

II. Experiment and simulation

Details of the photodiode structure can found in Ref.[4]. A short description is given here for the sake of completeness. The photodiode is manufactured using p-type high resistive silicon, and a positivitely charged oxide layer with charge density of $6.2\times10^{11}\,\mathrm{cm}^{-2}$ is grown using thermal oxidation. The photodiode junction is formed by the attraction of bulk electrons to the Si/SiO_2 interface [5].

Experimental measurements are performed with illumination from a power stabilized laser with wavelength of 488 nm.

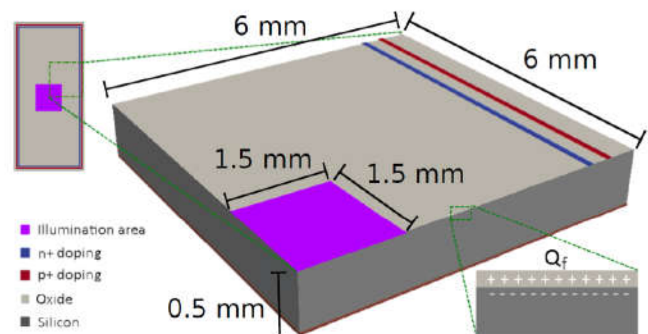

Fig. 1. Simulation structure with contacts (blue and red) and illumination area (purple). A schematic drawing is inserted to show the simulation structure relative to the whole photodiode. Furthermore, a schematic drawing of the interface structure with fixed and induced charges are shown.

Three laser power levels (250 µW, 750 µW and 1202 µW) are used, and these power levels are calculated from the photocurrent under an applied reverse bias voltage that provides a saturated response. Thus, only absorbed light is considered. Four-point probe is used for the I-V characterization, and the IQD is estimated with the assumption that the highest saturated photocurrent represents zero recombination loss of the photogenerated electron-hole (e-h) pairs.

The simulations are performed using the software Cogenda Genius with version 1.8.0 [6] and it iterates for a self-consistent solution between the Poisson's equation and the continuity equations for electrons and holes. Figure 1 shows the simulation structure. To reduce the computational demand, the simulation structure is truncated in its length, and the symmetry around the center is used. The illumination spot (highlighted in purple) is simplified to a spatially uniform square of 1.5 mm×1.5 mm. This area represents 1/4 of the illumination of the real experiment. Calculation of the IQD is performed by finding the ratio between the total photogenerated and recombinated e-h pairs, such that

$$IQD = \frac{R_{surf} + R_{bulk}}{G_{opt}}, \qquad (1)$$

where R_{surf} is the total surface recombination, R_{bulk} is the total bulk recombination and G_{opt} is the total concentration

978-1-5386-5599-3/18/$31.00 ©2018 IEEE

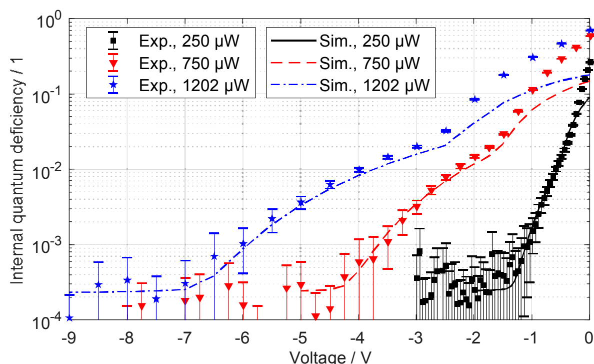

Fig. 2. Internal quantum deficiency as a function of applied reverse bias voltage at different laser power levels, showing both experimental and simulation results.

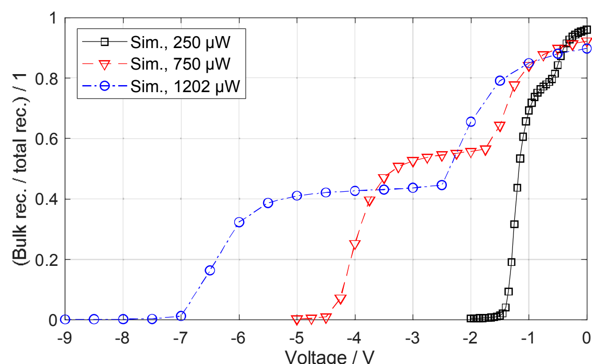

Fig. 3. The ratio between bulk recombination to the total recombination as a function of reverse bias voltage for different power levels. These curves are directly related to the simulated curves in Fig. 2.

of photogenerated e-h pairs. These values are integrated using the software ParaView with version 5.2.0-RC3 64-bit [7]. The Shockley-Read-Hall (SRH) bulk lifetime and the surface recombination velocity for electrons and holes are varied to fit the experimental data. The SRV and lifetime for holes are set to be equal to electrons.

III. Results and Discussions

Figure 2 shows the internal quantum deficiencies as a function of applied reverse bias voltage from the experiment and simulation. Focusing on the experimental data, the error-bars represent type-A uncertainty ($k = 1$) of the data point. It can be seen that the saturation of IQD requires increased reverse bias voltage for increased power levels. For power level of 750 μW and 1202 μW, a reverse bias voltage of -4.5 V and -7 V is required, respectively. For reverse bias voltages below the threshold voltage, the responsivity of the induced junction photodiode becomes non-linear and the loss components from recombination are very significant.

With a further decreased reverse bias voltage, both the experimental and the simulation results show a sudden increase in the gradient of the IQD. For power level of 750 μW and 1202 μW, this increase-point occurs at -1.8 V and -2.5 V, respectively. It is observed (not shown) that this behaviour is resulted by the added recombination components when the photogenerated minority carriers (electrons) are capable of reaching the rear-side. Apart from the low reverse bias voltage region with rear-side recombination, the fitting of the experimental curves performs quite well. Fortunately, the strategy of extracting surface recombination velocity (of the front side) and SRH bulk lifetime does not depend on rear-side.

Figure 3 shows the contribution of the bulk recombination as a function of voltage for the simulated curves in Fig. 2. Three plateaus can be identified and they are related to the three different mechanisms described in connection with Fig. 2. Concentrating on the middle plateau, it can be seen that the contribution from bulk recombination varies between different power levels in a monotonic trend. Practically, it means that a variation of the bulk lifetime and/or the surface recombination velocity will affect the IQD curves in a different magnitude depending on the laser power levels. This restricts the span of values that the bulk lifetime and the surface recombination velocity can possess. Thus, by fitting the experimental I-V curves in a region with significant recombination losses over multiple laser power levels, the bulk lifetime and surface recombination velocity can be determined. For this photodiode, the SRV and SRH bulk lifetime are fitted to be $7{\times}10^4$ cm/s and 1.8 ms, respectively. From Fig. 2, it can be seen that the lowest IQD is $\sim$230 parts per million.

IV. Conclusion

An induced junction photodiode has been characterized using I-V measurements under illumination with different laser power levels. The experimental results are fitted through internal quantum deficiencies using 3D device charge transfer simulations. The results show that the bulk lifetime and the surface recombination velocity for electrons and holes can be extracted when considering multiple laser power levels. Furthermore, it is revealed that only parts of the experimental I-V curve need to be taken into account for the extraction.

References

[1] J. Zwinkels et al. *Mise en pratique* for the definition of the candela and associated derived units for photometric and radiometric quantities in the International System of Units (SI), Metrologia, Vol. 37, 2016

[2] M. Sildoja et al., Reflectance calculations for a predictable quantum efficient detector, Metrologia, Vol. 46, S151-S154, 2009

[3] T. Dönsberg et al. Predictable quantum efficient detector based on n-type silicon photodiodes, Metrologia, Vol. 54, 2017

[4] M. Sildoja et al., Predictable quantum efficient detector: I. Photodiodes and predicted responsivity, Metrologia, Vol. 50, 385-394, 2013

[5] T. E. Hansen, Silicon UV-photodiodes using natural inversion layers, Physica Scripta, Vol. 18 471, 1978

[6] Genius semiconductor device simulator V1.7.4 manual, *http://www.cogenda.com/downloads/docs/genius_ug_en.pdf*

[7] Paraview Wiki, http://www.paraview.org/Wiki/ ParaView

[8] K. D. Stock et al. Lowest uncertainty direct comparison of a mechanically-cooled and a helium-cooled cryogenic radiometer, Metrologia, Vol. 37 437-439, 2000